

Supplementary Material

For

Open-Chain Crown-Ether-Derived Two-Photon Fluorescence Probe for Real-Time Dynamic Biopsy of Mercury Ions

Chibao Huang,^{A,E} Daohai Zhang,^B Junle Qu,^C Xiaonan Liu,^{D,E} Guanglian Zhao,^A Tingxiang Yuan,^A and Yang Liu^A

^a *Chemistry and Chemical Engineering College, Zunyi Normal University, Zunyi 563002, Guizhou, China*

^b *Research and Development Department (R & D), National Engineering Research Center for Compounding and Modification of Polymeric Materials, Guiyang, 55004, Guizhou China*

^c *Key Laboratory of Optoelectronic Devices and Systems of Ministry of Education and Guangdong Province, Shenzhen University, Shenzhen 518060, Guangdong, China*

^d *The Hospital Infection Management Section, the Affiliated Baiyun Hospital of Guizhou Medical University, Guiyang, 550014, Guizhou China*

E-mail: huangchibao@163.com; liuxiaonan309@163.com

Spectroscopy Data:

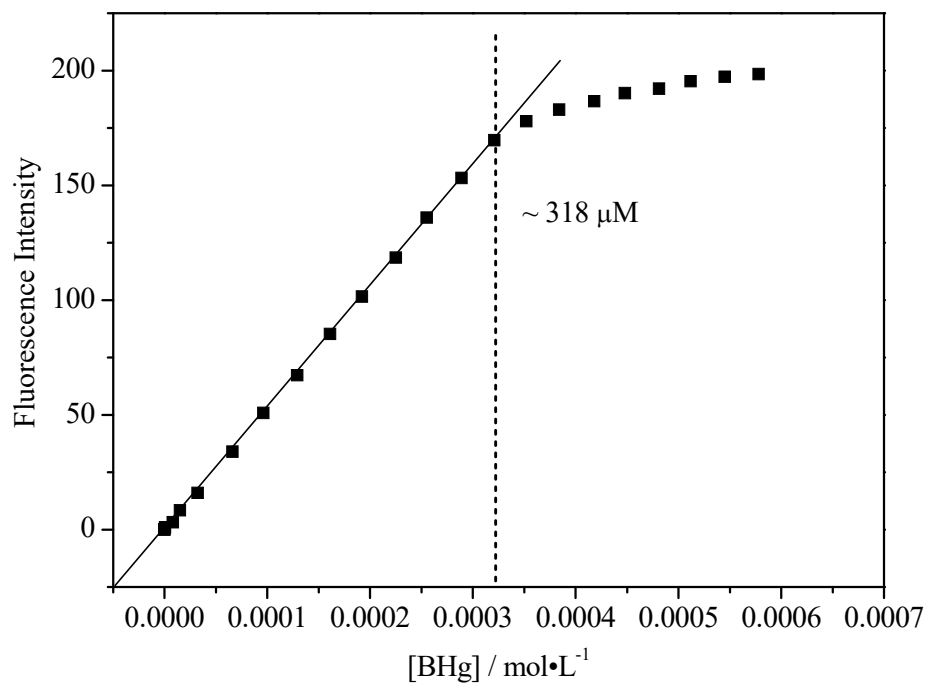


Fig. S1 Plot of one-photon fluorescence intensity against probe concentration for **BHg** in H₂O. The excitation wavelength was 467 nm.

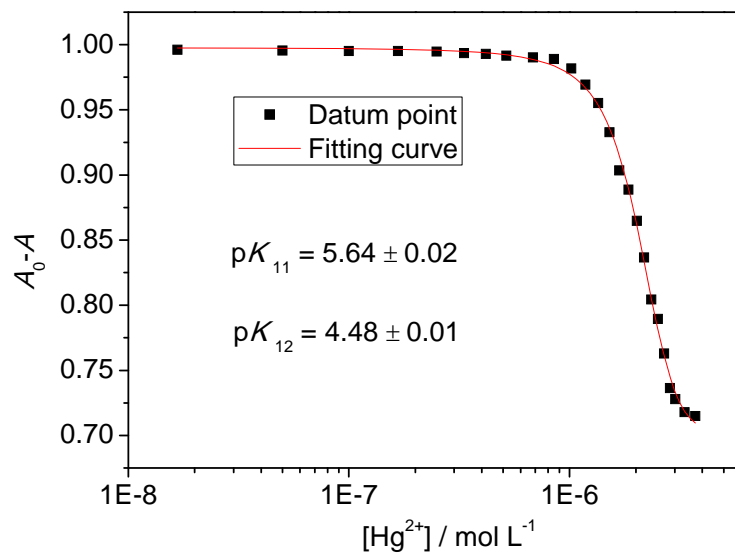


Fig. S2 The best fitting curve between Changes in one-photon absorption intensities of **BHg** ($10.0 \mu\text{M}$) at 467 nm and mercury ion concentrations. These data were measured in 30 mM MOPS buffer (100 mM KCl, 10 mM EGTA, $\text{pH } 7.2$).

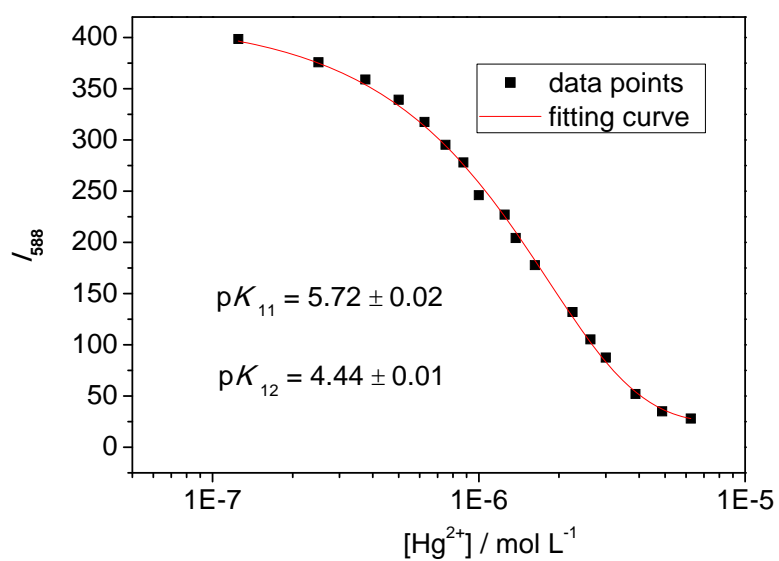


Fig. S3 The best fitting curve between Changes in one-photon emission intensities of **BHg** ($1.0 \mu\text{M}$) at 588 nm and lead ion concentrations. These data were measured in 30 mM MOPS buffer (100 mM KCl, 10 mM EGTA, pH 7.2).

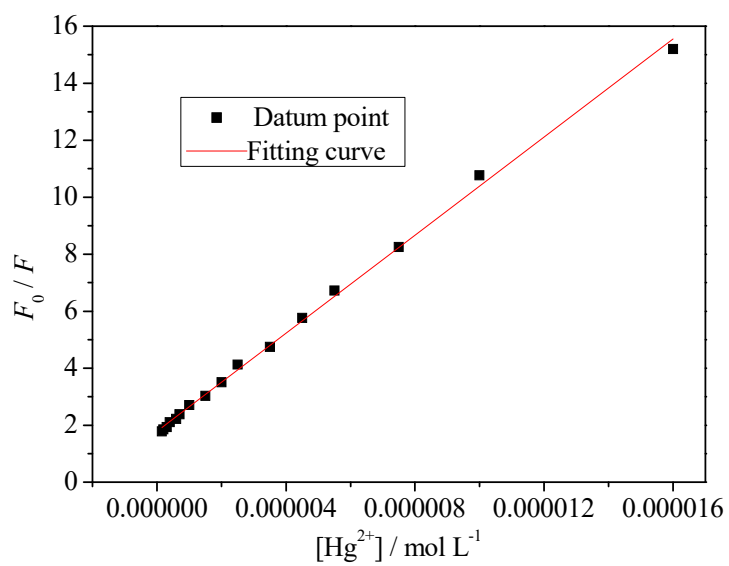


Fig. S4 The best fitting curve between the OPF intensities for **BHg** ($1.0 \mu\text{M}$) at 588 nm and the Hg^{2+} concentrations from 1.0×10^{-7} to $1.6 \times 10^{-5} \text{ mol L}^{-1}$.

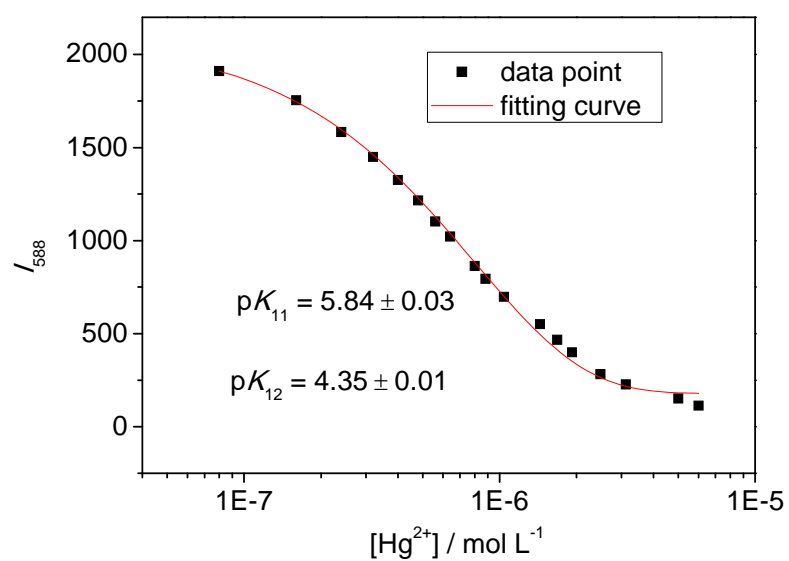


Fig. S5 The best fitting curve between Changes in two-photon emission intensities of **BHg** ($1.0 \mu\text{M}$) at 588 nm and lead ion concentrations. These data were measured in 30 mM MOPS buffer (100 mM KCl, 10 mM EGTA, pH 7.2).

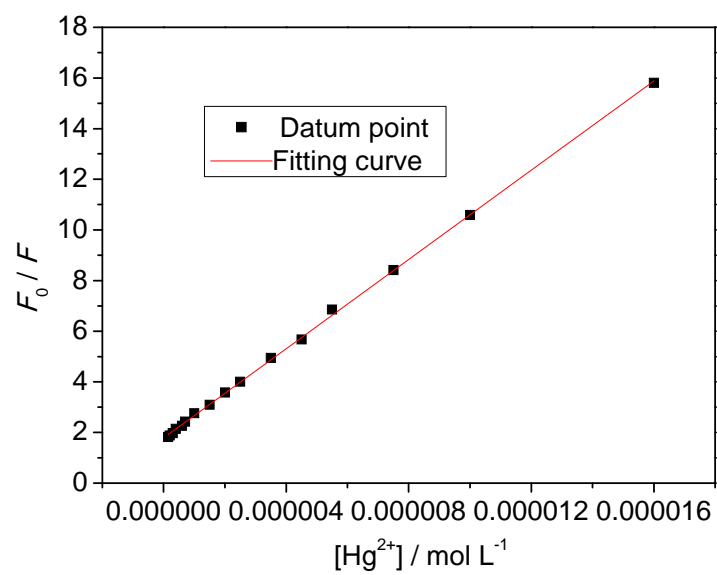


Fig. S6 The best fitting curve between the TPF intensities for **BHg** ($1.0 \mu\text{M}$) at 588 nm and the Hg^{2+} concentrations from 1.0×10^{-7} to $1.6 \times 10^{-5} \text{ mol L}^{-1}$.

Job's plot for **BHg**–**Pb**²⁺ complex

Solutions of **BHg** and **Hg**²⁺ in H₂O (30 mM MOPS, 100 mM KCl, 10 mM EGTA, pH 7.2) at different mole fractions were prepared by mixing **BHg** and **Hg**²⁺ in H₂O (30 mM MOPS, 100 mM KCl, 10 mM EGTA, pH 7.2) in appropriate ratios while maintaining the total concentration to 1 μ M. The emission of each solution at 588 nm was measured. The concentration of **BHg**–**Hg**²⁺ complex for each solution was calculated by using the fluorescence emission data and the binding constants (Fig. S3 and S4). The plot of [complex] vs the mole fraction of **Hg**²⁺ shows a maximum when the mole fraction is 0.67, indicating the formation of a 1:2 complex (Fig. S7).

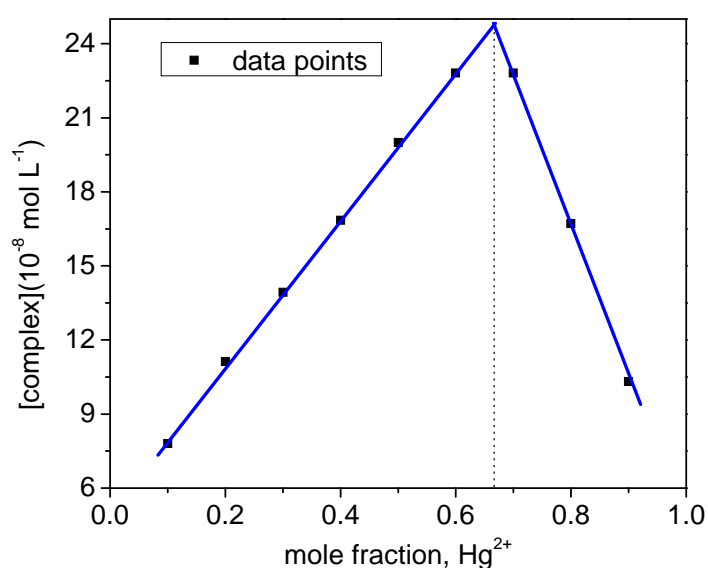


Fig. S7 Job's plot for the complexation of **BHg** with **Hg**²⁺ in 30 mM MOPS buffer (100 mM KCl, 10 mM EGTA, pH 7.2).

The TPF intensities for BHg (1.0 μM) at 587 nm versus the Hg^{2+} concentrations

Table 1 Relative TPF intensities of BHg (1.0 μM) at 587 nm under different Hg^{2+} concentrations.

Serial number	X ^a	Y ^b
1	1.00E-07	720
2	1.50E-07	680.32
3	2.00E-07	635.12
4	3.00E-07	601.89
5	4.00E-07	550.38
6	6.00E-07	511.45
7	7.00E-07	496.51
8	1.00E-06	438.21
9	1.50E-06	386.54
10	2.00E-06	340.09
11	2.50E-06	298.47
12	3.50E-06	257.78
13	4.50E-06	217.28
14	5.50E-06	185.98
15	7.50E-06	155.46
16	1.00E-05	125.75
17	1.25 E-05	100.00
18	1.40 E-05	70.00
19	1.60 E-05	40.00

^a $[\text{Hg}^{2+}] / \text{mol L}^{-1}$
^b Relative TPF Intensity

Cell Culture.

Mouse fibroblast was cultured in DMEM (HyClone) supplemented with 10 % FBS (Invitrogen), penicillin (100 units / mL), and streptomycin (100 μ g / mL). Two days before imaging, the cells were passed and plated on glass-bottomed dishes (MatTek). For labeling, the growth medium was removed and replaced with DMEM without FBS. The cells were treated and incubated with 1 μ M sensor at 37 °C under 5 % CO₂ for 30 min. The cells were washed three times with phosphate buffered saline (PBS; Invitrogen) and then imaged after further incubation in colorless serum-free media for 15 min.

Preparation and Staining of mouse brain tissue slices. Slices were prepared from the brain tissues of a mouse. Preparation and staining of mouse brain tissue slices have been conducted in the same way as described in the literature [S1].

References

- (S1) Kim, H. M.; Seo, M. S.; An, M. J.; Hong, J. H.; Tian, Y. S.; Choi, J. H.; Kwon, O.; Lee, K. J.; Cho, B. R. *Angew. Chem. Int. Ed.* **2008**, *47*, 5167

NMR Spectra:

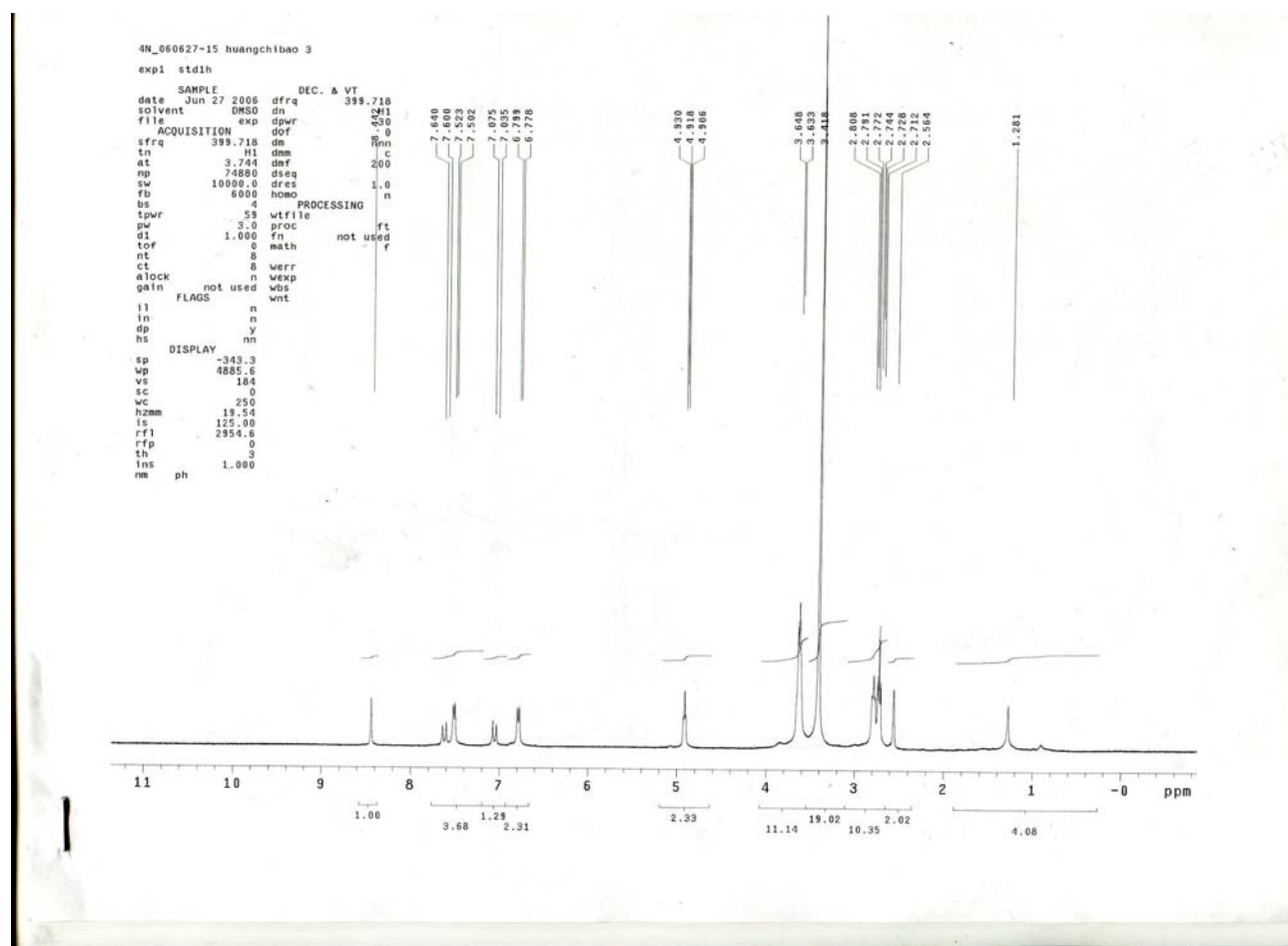


Fig. S8 ^1H NMR spectrum for compound **BHg** in $\text{DMSO-}d_6$

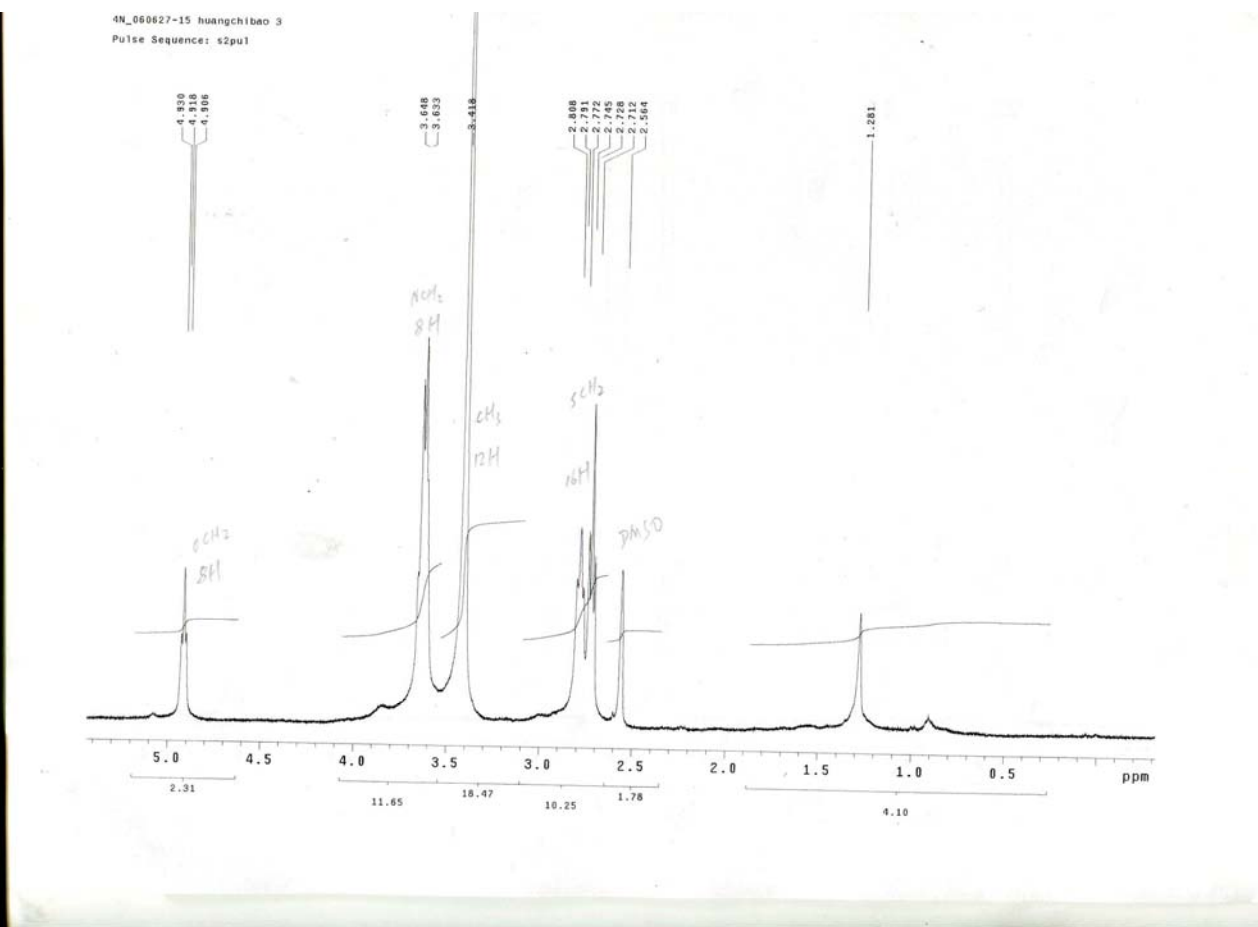
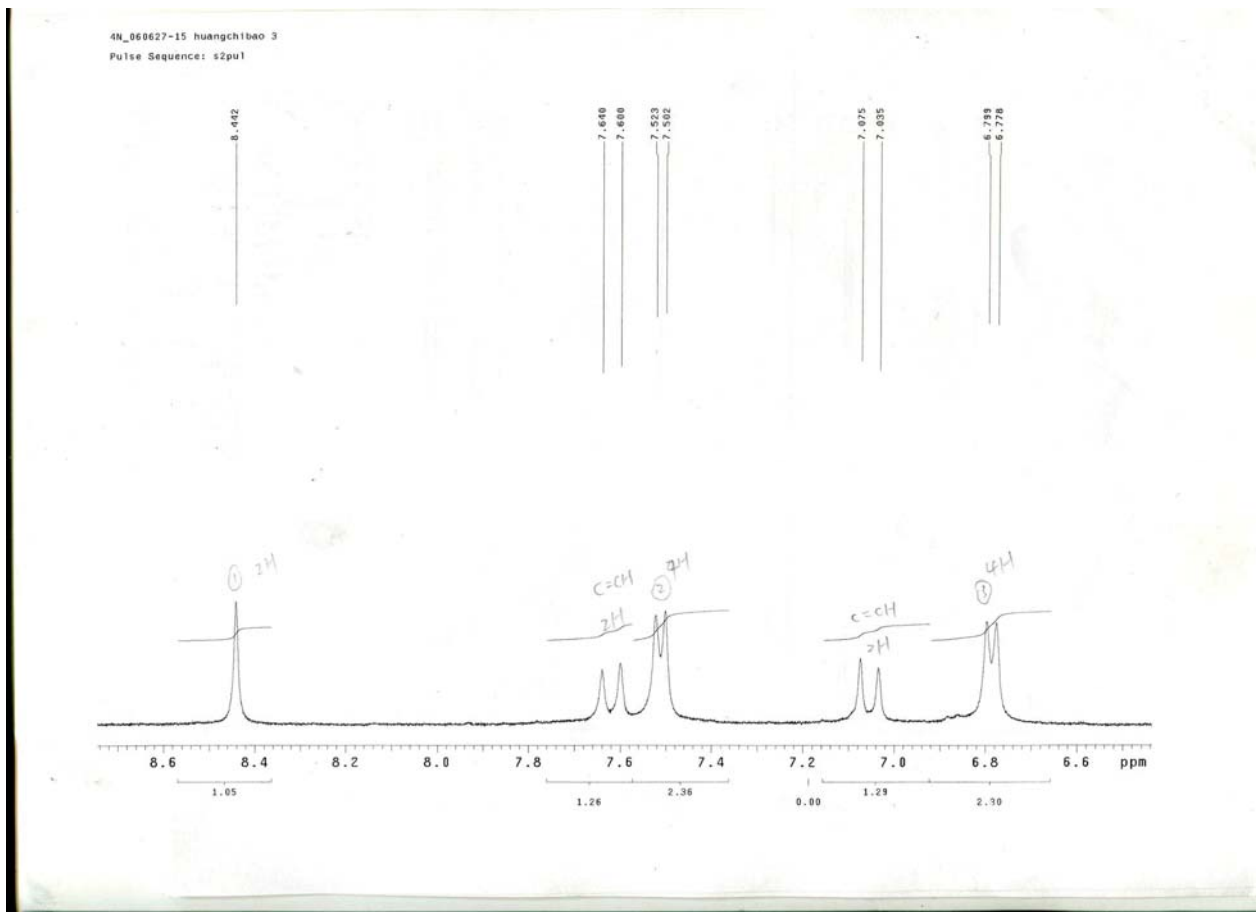
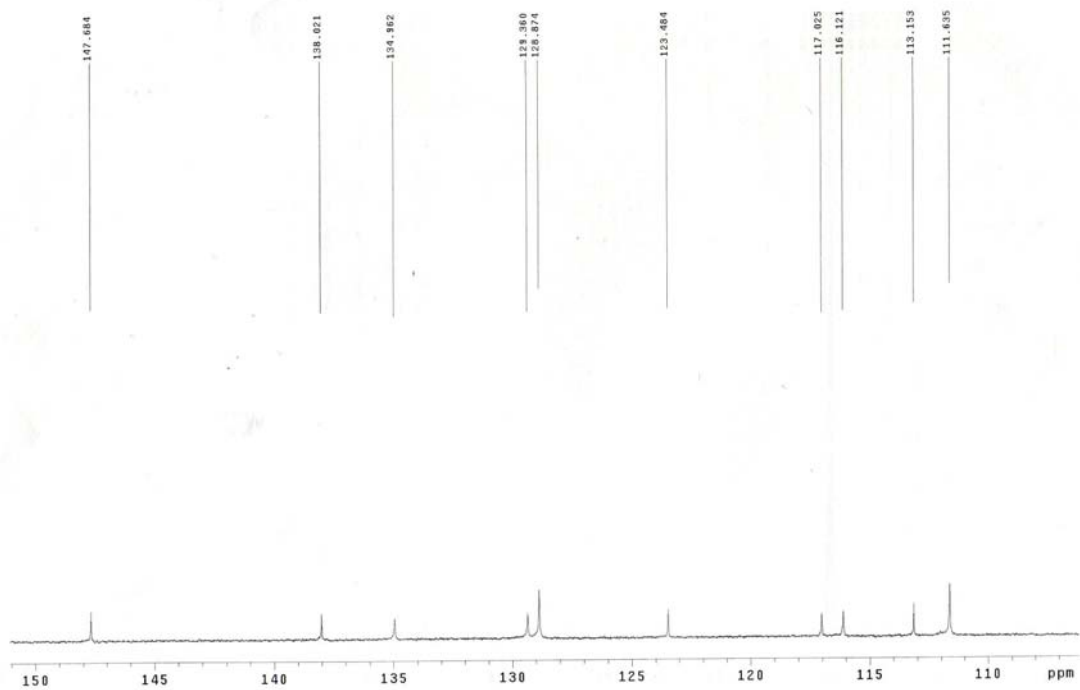


Fig. S9 ^1H NMR spectrum for compound **BHg** in $\text{DMSO-}d_6$

4N_060630-25 huangchibao 3
Pulse Sequence: s2pu1



4N_060630-25 huangchibao 3
Pulse Sequence: s2pu1

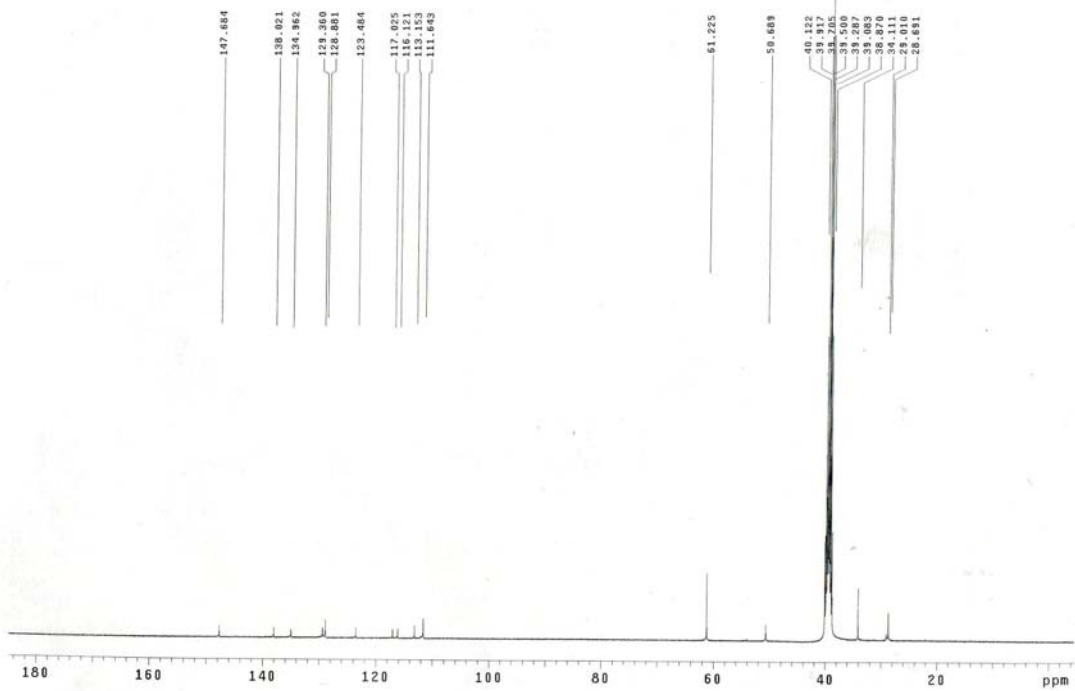


Fig. S10 ¹³C NMR spectrum for probe **BHg** in DMSO-*d*₆

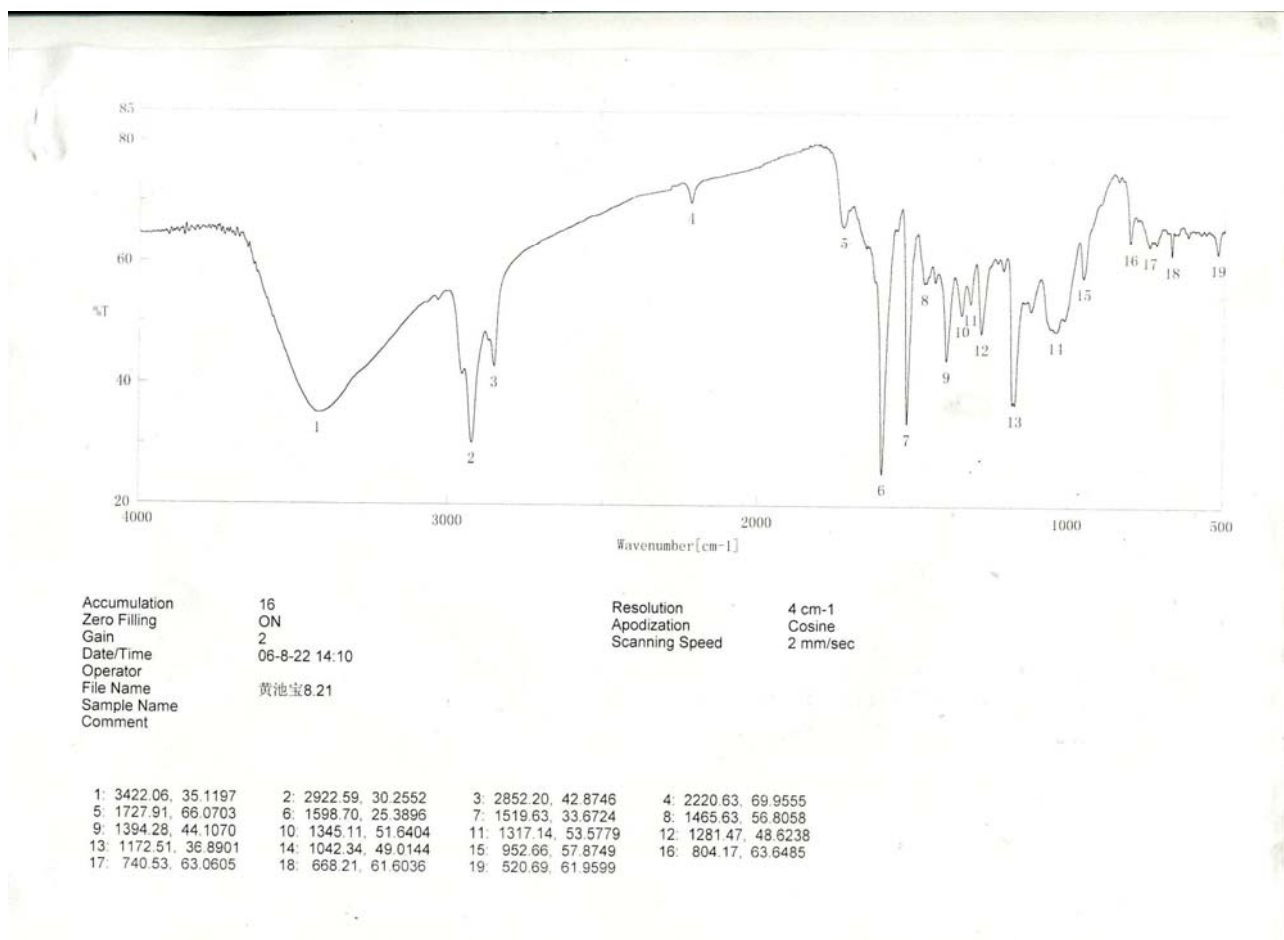


Fig. S11 The infrared spectrum for probe **BHg**

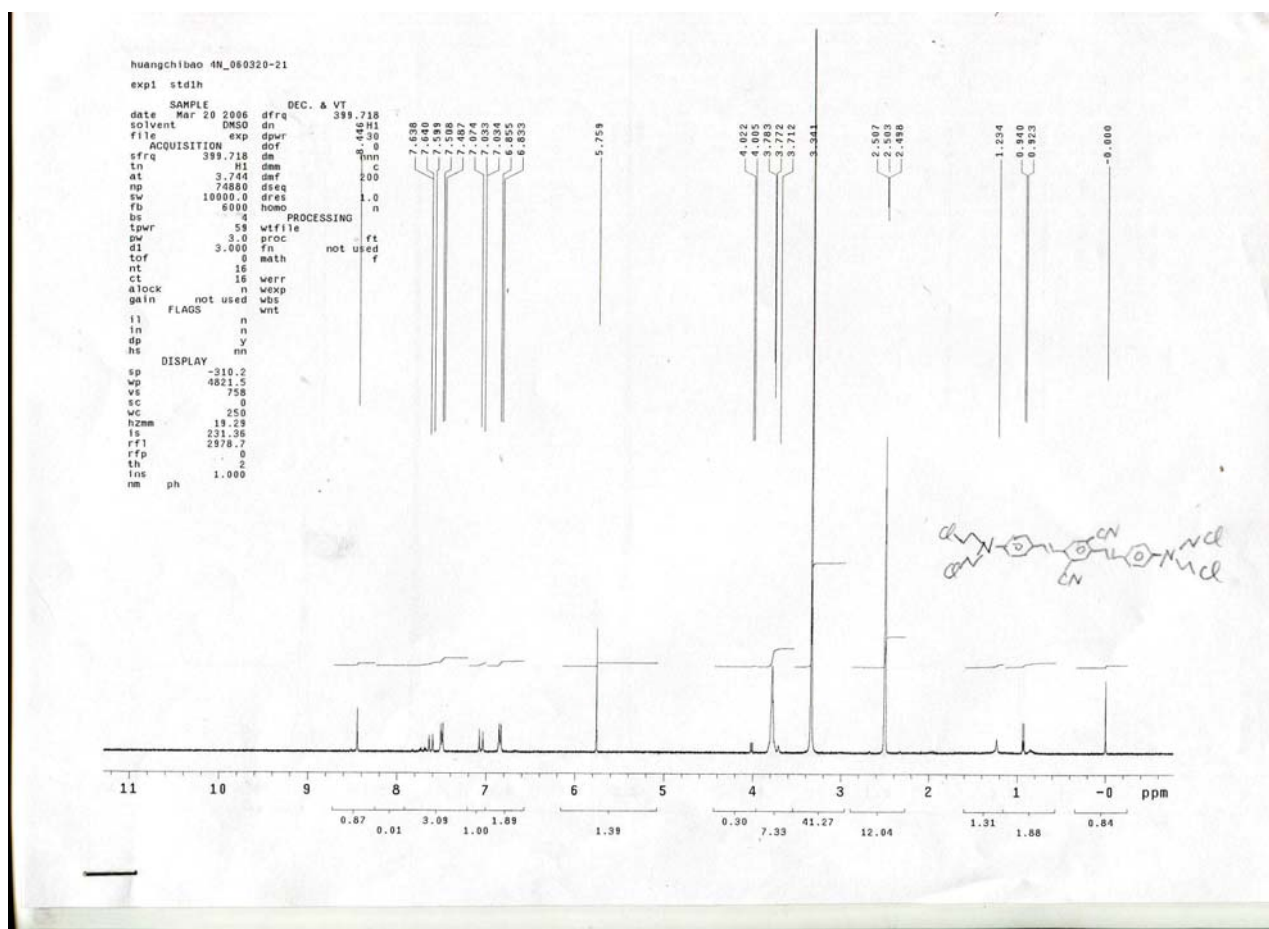


Fig. S12 ^1H NMR spectrum for compound **8** in $\text{DMSO-}d_6$

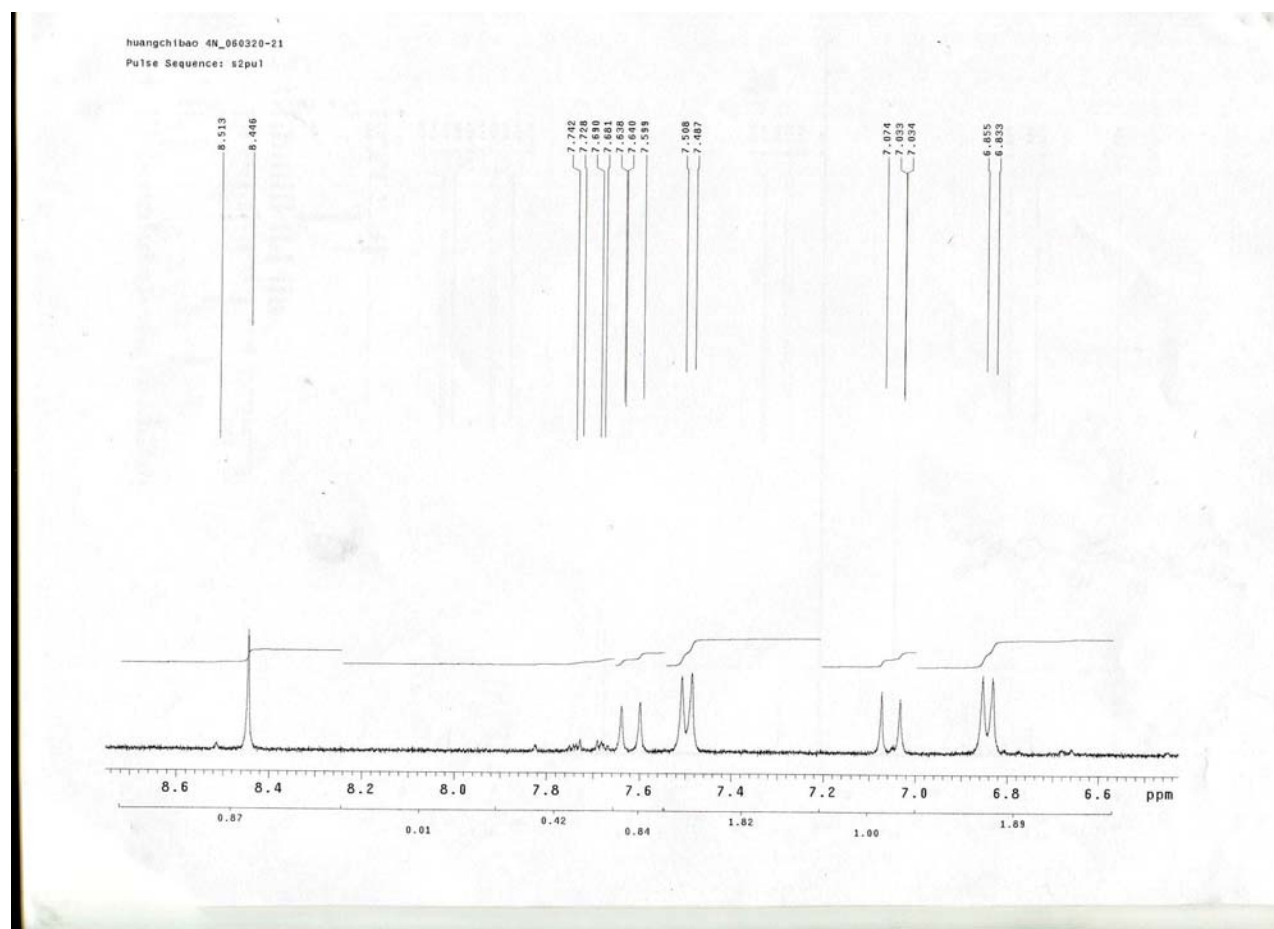
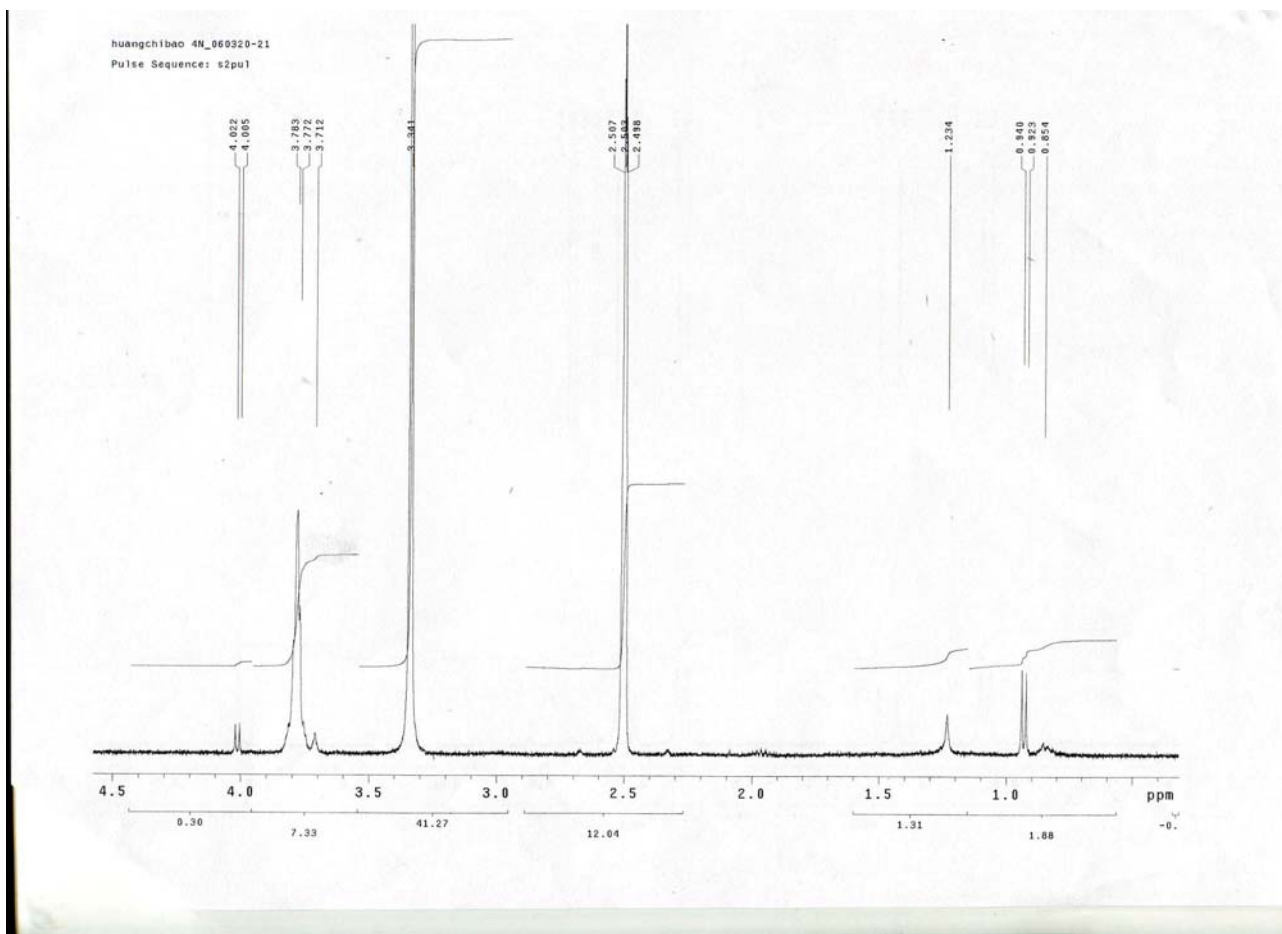


Fig. S13 ^1H NMR spectrum for compound **8** in $\text{DMSO-}d_6$